AIChE

Kinetic Study of the Decomposition of 2-Butanol on Carbon-Based Acid Catalyst

J. Bedia, R. Ruiz-Rosas, J. Rodríguez-Mirasol, and T. Cordero
Chemical Engineering Dept., School of Industrial Engineering, University of Málaga, Campus de Teatinos, 29071 Málaga, Spain

DOI 10.1002/aic.12056
Published online October 28, 2009 in Wiley InterScience (www.interscience.wiley.com).

The catalytic conversion of 2-butanol on a carbon-based acid catalyst prepared by chemical activation of olive stone with phosphoric acid was investigated. The carbon catalyst showed a considerable amount of surface phosphorus, presumably in form of phosphate groups, as revealed by XPS, despite a washing step carried out after the activation process. Conversion of 2-butanol yields mainly dehydration products, mostly cis-2-butene and trans-2-butene with lower amounts of 1-butene, and a very small amount of mek as dehydrogenation product. Kinetic interpretation of the experimental data was performed using two elimination mechanisms for the dehydration reaction; an E1-mechanism (two-step mechanism) and an E2-mechanism (one-step mechanism). The rate expressions derived from both models fit properly the experimental results, suggesting that probably the two mechanisms occur simultaneously. This is supported by the similar rate constant obtained for the formation of the carbocation and the olefins in the E1 and E2 mechanisms, respectively. © 2009 American Institute of Chemical Engineers *AIChE J,* 56: 1557–1568, 2010

Keywords: catalysis, Activated carbon, reaction kinetics, 2-butanol, dehydration

Introduction

Biomass contains almost negligible amount of nitrogen, sulfur and metals and, thus, represents an interesting alternative raw material for the oil production from an environmental point of view. Flash pyrolysis of biomass produces liquid oil (bio-oil) of great interest as fuel, constituted mostly by oxygenated compounds.[1,2] However, transformation of bio-oil is necessary to reach a quality similar to that of the conventional fuel. Studies have been conducted to improve the quality of bio-oil as fuel through catalytic processes with inorganic acid solids.[3,4,5] Gayubo et al.[4] studied the catalytic transformation of several model components of biomass pyrolysis oil, such us phenols and alcohols (1 and 2-propanol, 1 and 2-butanol…), over HZSM-5 zeolite obtaining mainly light olefins and aromatics.

Correspondence concerning this article should be addressed to J. Rodríguez-Mirasol at mirasol@uma.es.

Different inorganic catalyst have been used in alcohol decomposition reaction, such us, noble metal-based materials,[6,7] transition metal oxides,[8,9] zeolites,[10,11] ion-exchange resins[12,13] and amorphous phosphates[14] among others. Intramolecular dehydration over acid catalysts, can either proceed as a two-step mechanism (E1) or as a one-step concerted mechanism (E2). There exists a third possibility, a two-step process over basic catalysts (the E1cb mechanism). In this case, the intermediate is a negative charged specie, carbanion. The three mechanisms are very similar each other, with the only difference in the order in which the cleavage of the C-O bond and deprotonation takes place.[15] The alcohol decomposition reaction mechanism is a function of the type of catalyst, the acidity of the catalyst and the stability of the carbocation formed.[14,16,17]

The use of activated carbons in catalysis has grown continuously in the last decade due to their properties as support and/or because they can play a role as catalysts per se.[18,19,20] Carbon materials can be used as catalysts for acid/base reactions because of the presence of surface oxygen groups of acidic and/or basic character.[21,22,23] To increase the surface

acidity of carbon catalysts for alcohol decomposition reactions, the carbons were usually oxidized in a supplementary step with different chemical compounds in order to introduce oxygen surface complexes of acidic character.[24,25,26] This increase in the surface acidity is associated with the formation of carboxylic and lactonic groups, which show a low to moderate thermal stability.[27] Chemical activation with phosphoric acid results in carbons with high surface acidity as a consequence of the oxygen-phosphorus groups formed on the carbon surface during the activation process.[28,29,30] Furthermore, these acid groups have shown a high stability in the presence of water vapor (up to 10%vol.) for the catalytic dehydration of 2-propanol[30] which is very important for the valorization of oxygenates from biomass usually with high-water content. The acid groups of the carbons obtained by this single and direct way show a high-thermal stability decomposing at temperatures higher than 700 °C.[28,29,30] Carbons also show a high-structural hydrothermal stability. This constitutes an important advantage with respect to inorganic catalysts, like zeolites, which suffer an irreversible deactivation due to the deterioration of their crystalline structure in the presence of water at moderate to high-temperatures.[31]

In this work, we examine the decomposition (dehydration and dehydrogenation) of 2-butanol (as model compound of bio-oil) in order to obtain light olefins by using an acid activated carbon catalyst obtained by chemical activation of olive stone waste with H_3PO_4. A kinetic study of the 2-butanol decomposition on the acid carbon is also presented in which two mechanisms (E1 and E2) for dehydration reaction and an E2 mechanism for dehydrogenation reaction, in two different models, have been analyzed. The corresponding kinetics and thermodynamics parameters were obtained.

Experimental

Catalyst preparation

The activated carbon catalyst was obtained from olive stone residues. The ash content of the olive stone is 0.42%. The precursor was impregnated with 85% (w/w) aqueous H_3PO_4 solution at room temperature and dried for 24 h at 333 K in a vacuum dryer. The impregnation ratio (weight of H_3PO_4 relative to that of dry precursor) was 1. The impregnated sample was activated under continuous N_2 flow (150 cm^3 STP/min) in a conventional tubular furnace. The activation temperature was reached at a 10 K/min heating rate and maintained for 2 h at 773 K. The activated sample was cooled inside the furnace, maintaining the N_2 flow and then washed with distilled water at 333 K until neutral pH and negative phosphate analysis in the eluate.[32] The resulting carbon catalyst was dried at 383 K. The yield of the activation process is 43.3%.

Catalyst characterization

The porous structure of the catalyst was characterized by N_2 adsorption-desorption at 77 K performed in an Omnisorb 100cx model of Coulter and by CO_2 adsorption at 273 K, carried out in an Autosorb-1 model of Quantachrome. The sample was previously outgassed during at least 8 h at 423 K. From the N_2 adsorption-desorption isotherm, the apparent surface area (A_{BET}^{N2}) was determined applying the BET equation,[33] the micropore volume (V_t^{N2}), and the external surface area (A_t^{N2}) were calculated using the t-method,[34] and the mesopore volume (V_{mes}^{N2}) was determined as the difference between the adsorbed volume at a relative pressure of 0.95 and the micropore volume (V_t^{N2}).[35] The narrow micropore surface area (A_{DR}^{CO2}), and micropore volume (V_{DR}^{CO2}) were obtained by the Dubinin-Radushkevich (DR) method[36] applied to the CO_2 adsorption isotherm. N_2 and CO_2 molecular areas of 16.2 $Å^2$ [37] and 18.7 $Å^2$ [38], respectively, were used.

The surface chemistry of the sample was analyzed by temperature-programmed desorption (TPD) and X-ray photoelectron spectroscopy (XPS). TPD profiles were obtained in a custom quartz tubular reactor placed inside an electrical furnace. The sample was heated from room-temperature up to 1173 K at a heating rate of 10 K/min in a helium flow (200 cm^3 STP/min). The amounts of CO and CO_2 desorbed were monitored with nondispersive infrared (NDIR) gas analyzers (Siemens ULTRAMAT 22). X-ray photoelectron spectroscopy (XPS) analyses of the sample were obtained using a 570°C model physical electronics apparatus, with MgKα radiation (1253.6 eV). For the analysis of the XPS peaks, the C1 s peak position was set at 284.5 eV and used as reference to position the other peaks.[39,40] The fitting of the XPS peaks was done by least squares using Gaussian-Lorentzian peak shapes.

The total acidity and acid strength distribution of the catalyst were determined by temperature programmed desorption of ammonia. The NH_3-TPD was performed using 80 mg of catalyst saturated with NH_3 for 5 min at 373 K. After saturation, the NH_3 weakly adsorbed was desorbed in a He flow, at the adsorption temperature, until no NH_3 was detected in the outlet gas. The NH_3-TPD was performed by raising the temperature up to 773 K at a heating rate of 10 K/min. The NH_3 was measured by gas chromatography using a thermal conductivity detector.

2-butanol decomposition

The catalyst activities were measured by the decomposition of 2-butanol performed at atmospheric pressures, in a quartz fixed bed microreactor (4 mm i.d.) placed inside a vertical furnace with temperature control. 100 mg of catalyst (100–300 μm particle size) was dispersed in 1 g of quartz (100–300 μm) to avoid thermal gradients in the bed. A nitrogen stream was saturated with 2-butanol vapor by contact in a saturator system with liquid 2-butanol at temperatures between 283 and 303 K, resulting in partial pressures from 0.0085 up to 0.0340 atm. The 2-butanol used was of analytical grade purity (Fluka, puriss p.a. $\geq$ 99.5%). To prevent condensation of 2-butanol and its reaction products, all the connections, from the saturator to the chromatograph, were heated by a wired resistance above 393 K. The gas reaction mixture was fed to the reactor at total flow rates between 50 and 200 cm^3 STP/min (space times, $W/F_{But2OHo} = 0.042$–0.170 g·s/μmol). Analysis of reactant and products was done using online gas chromatography (PerkinElmer Autosystem GC, 50 m HP-1 methyl silicone capillary column, flame ionization detector). The temperature program of the chromatography column was 50°C for the first 4 min followed by a heating to 150°C at a heating rate of 20°C/min.

The reaction rate, r, was defined as the mol amount of 2-butanol transformed in 1 s per gram of catalyst. The conversion was defined as the molar ratio of 2-butanol converted to 2-butanol feeded to the reactor. The selectivity was defined as the molar ratio of a given product to that of the total product formed. The carbon balance was reached with an error lower than 5%.

Results and Discussions

Catalyst characterization

The catalyst used in this work was an activated carbon obtained by chemical activation of olive stone with H_3PO_4, with particle size of 100–300 μm. The ash content of the carbon is lower than 0.5 wt %. This is due to the very low ash content of olive stone (0.42 wt %), and the relatively high yield of the activation process (43.3 wt %). Furthermore, during the washing of the phosphoric acid most of the inorganic matter of the carbon is removed. This way, the purity of the activated carbon is high and only phosphorus from the activation process is observed at a significant content. The physicochemical properties of the fresh catalyst are presented in Table 1. The data presented are referred to structural parameters obtained from the N_2 adsorption-desorption and CO_2 adsorption isotherms, surface atomic concentration obtained by XPS and surface acidity of the carbon obtained by adsorption, desorption and TPD of ammonia. The chemical activation of olive stone with H_3PO_4 produces an activated carbon with a wide microporous structure and a high apparent surface area (902 m^2/g), higher than those corresponding to other acid catalysts reported in the literature.[8,41,42] The higher value of A_{BET} with respect to that of A_{DR} indicates the existence of a wide microporous structure.[43] The carbon catalyst presents also a relatively high value of the external surface area A_s, of 113 m^2/g, which is important in catalytic applications. The surface area and porosity data reveal that the catalyst prepared is a solid with essentially a wide microporous structure.

The mechanism of olive stone activation with H_3PO_4 to produce activated carbons seems to proceed through formation of phosphate and polyphosphate bridges that connect crosslink biopolymer fragments, avoiding the contraction of the structure by the effect of temperature. Part of the activating agent is removed during the washing step, leading to a carbon matrix in an expanded state with an accessible pore structure.[32,44] According to XPS analysis the surface of the carbon studied in this work shows a significant amount of P (4.35 wt %). Taking into account that the ash content of the olive stone used as raw material is relatively low (0.42 wt %, and only 25 wt % of this ash is phosphorus), the yield of the activation process is 43.3 wt % and that during the washing of the phosphoric acid most of the inorganic matter is removed, we could estimate that the amount of phosphorus coming from the olive stone in the resulting activated carbon should be almost negligible. Furthermore, there are references[30,45] in the technical literature confirming that phosphorus is intercalated in the carbon matrix during the chemical activation with phosphoric acid. Therefore, part of the phosphorus of the activating agent remains on the carbon surface after the washing step, presumably in form of phosphate groups, resulting in acid activated carbons.[46,47] Therefore, we could conclude that the surface phosphorus of the resulting carbon comes from the activation process and not from the raw material. The XPS P2p of the carbon catalyst shows two bands at 134.0 and 133.4 eV, suggesting the presence of C-O-PO_3 (134.0 eV) and C-PO_3 (133.4 eV) groups on the surface of the catalyst,[28,30] with a higher contribution of the C-O-PO_3 groups on the carbon surface.[28,30,48] The P-OH groups of these surface phosphates act as Brönsted acid site and may play an important role on the acid character of the carbon catalyst prepared in this work.

Table 1. Porous Structure and Chemical Properties of Fresh Catalyst

Surface area and porosity	
77 K N_2 adsorption	
A_{BET}^{N2} (m^2/g)	902
V_{mic}^{N2} (cm^3/g)	0.384
V_{mes}^{N2} (cm^3/g)	0.120
A_t^{N2} (m^2/g)	113
273 K CO_2 adsorption	
A_{DR}^{CO2} (m^2/g)	613
V_{DR}^{CO2} (cm^3/g)	0.233
Surface atomic concentration obtained by XPS (w%)	
C1s	82.28
O1s	13.14
N1s	0.23
P2p	4.35
CO_2 and CO evolved from TPD	
Total CO_2 (μmol/g)	135
Carboxylic acids	10
Lactones	32
Anhydrides	86
Total CO (μmol/g)	1398
Anhydrides	88
Phenolic	340
Carbonyl and Quinone	970
Acidity, determined by adsorption and desorption and TPD of ammonia	
Total (μmol NH_3/g)	956
Weak (μmol NH_3/g)	390
Moderate (μmol NH_3/g)	303
Strong (μmol NH_3/g)	263

TPD provides information on the nature of the carbon-oxygen surface groups. Carboxylic acid and lactone groups evolve as CO_2 upon heating and carboxylic anhydride produce both CO_2 and CO, whereas desorption of CO derives from decomposition of phenol, ether and carbonyl/quinone surface groups.[27,49,50,51] Table 1 summarizes the amount of CO and CO_2 evolved from a TPD experiment for the catalyst used in this work, which correspond to different carbon-oxygen surface groups. The results of the TPD experiments reveal that the amount of CO evolved exceeds considerably that of CO_2, (1398 μmol/g of CO vs. 135 μmol of CO_2/g), suggesting that most of the carbon-oxygen groups present in the carbon are of non acidic nature (carbonyl and quinone) and esther phosphate groups. Phenolic hydroxyl groups evolve as CO and behave as a weak acid (340 μmol/g of CO calculated from TPD as phenolic group versus 390 μmol of NH_3/g calculated as weak acidic group by ammonia adsorption). The results obtained from NH_3-TPD suggest that the main part of the surface acidity of moderate and strong character (303 and 263 μmol of NH_3/g, respectively) corresponds

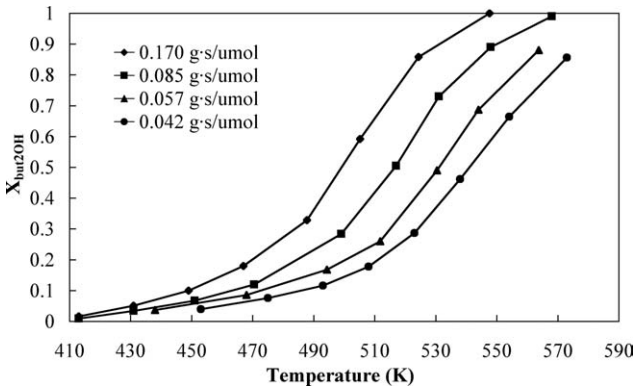

Figure 1. Conversion of 2-butanol, X_{But2OH}, as a function of reaction temperature at different $W/F_{But2OHo}$ with a constant partial pressure of 2-butanol, $P_{But2O}H = 0.017$ atm.

to H-phosphate groups formed in the carbon surface during the activation process, since weak acidic groups can be related with the amount of phenol groups.

A total acidity surface of 956 μmol NH_3 per gram of activated carbon was determined by ammonia adsorption-desorption-TPD. This value is high if compared with other acid catalysts described in the literature.[14,52,53] The high-surface acidity may be ascribed to the presence of phosphate groups on the surface of the carbons.

2-butanol decomposition

Decomposition of 2-butanol was studied on the carbon catalyst prepared by chemical activation of olive stone with phosphoric acid in a fixed-bed reactor. In the absence of catalyst, no reaction occurred below 750 K. Decomposition of 2-butanol on the carbon catalyst takes place in the temperature range from 413 to 573 K, at temperatures well bellow the region where homogeneous decomposition occurs.

The value of L_b/d_p (being L_p the bed length, and d_p the particle diameter) was 100, which indicates that axial dispersion can be considered negligible.[54,55,56] The absence of external and internal mass-transfer limitations for the decomposition of 2-butanol on the carbon catalyst in the fixed-bed reactor at the experimental conditions was checked theoretically. The effect of the external mass-transfer limitation was evaluated using the Damköhler number (Da), and the interphase external effectiveness factor (η_{ext}) was taken into account to evaluate the influence of external mass transport on the global reaction rate.[57] Values of Da and η_{ext} of $2.719 \cdot 10^{-2}$ and 0.974 were obtained, respectively. Internal mass-transfer limitation was evaluated using the isothermal intraphase internal effectiveness factor η, which is a function of the Thiele modulus ϕ.[57] Values of 0.834 and 0.957 were obtained for the Thiele modulus and the internal effectiveness factor, respectively. The values obtained for these parameters indicate that external and internal mass-transfer limitations may be considered negligible.

Figure 1 shows the steady-state conversion of 2-butanol, X_{But2OH}, vs. reaction temperature at different space times ($W/F_{But2Oho}$) with a constant inlet partial pressure of 2-butanol, $P_{But2OH} = 0.017$ atm. The steady-state conversion of 2-butanol was reached at about 30 min, and increases with increasing space time at a constant temperature. At the experimental conditions used in this study, complete conversion of 2-butanol is reached at temperatures between 543 and 580 K, depending on the space time.

Figure 2 presents the conversion of 2-butanol as a function of inlet partial pressure for different reactions temperatures. At a constant temperature, conversion of 2-butanol, practically, remained constant for different partial pressures of 2-butanol in the feed stream.

For all the experiments, selectivities were measured for the steady-state conversions (at approximately 30 min of time on stream (TOS)). Figure 3a shows that selectivities for all the products remained constant at temperatures higher than 508 K. The main products are 2-butenes (cis and trans isomers) and 1-butene. Only at low-temperature, bellow 500 K, the selectivity to mek is significant. Selectivities are not affected, significatively, by the inlet partial pressure of 2-butanol at constant temperature (Figure 3b).

The carbon catalyst is active for the dehydration of 2-butanol from 413 to 573 K yielding olefins, although formation of a small quantity of methyl ethyl ketone (mek) by dehydrogenation is sometimes observed, especially at high 2-butanol conversions. No secbutyl ether was detected as reaction product. Generally, bimolecular dehydration reactions of secondary or tertiary alcohols leading to ethers are very slow compared with monomolecular dehydration reactions yielding alkenes, particularly at low-alcohol partial pressures.[58,59] At the temperature range studied in this work, only four reactions products were detected (Figure 4), 1-butene, cis-2-butene and trans-2-butene from dehydration reaction and methyl ethyl ketone from dehydrogenation. All of them are elimination products and no skeletal isomerisation or cracking products were detected.

2-butanol dehydration to olefins is an elimination reaction. The formation of 1-butene, cis-2-butene and trans-2-butene and their distribution depend on the acid–base properties of the catalysts. The equilibrium cis/trans ratio is 0.59. A value close to this one indicates that the process of dehydration is thermodynamically controlled. In our case, a ratio value of 1.1 has been obtained, indicating that the process

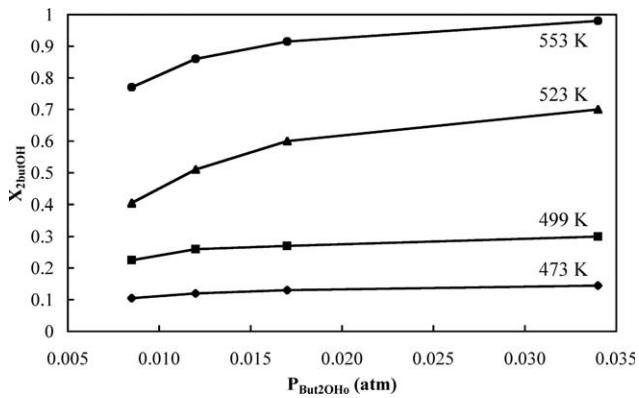

Figure 2. Conversion of 2-butanol, X_{But2OH}, as a function of P_{But2OH} at different reaction temperatures and constant $W/F_{But2OHo}$ (0.085 g·s/μmol).

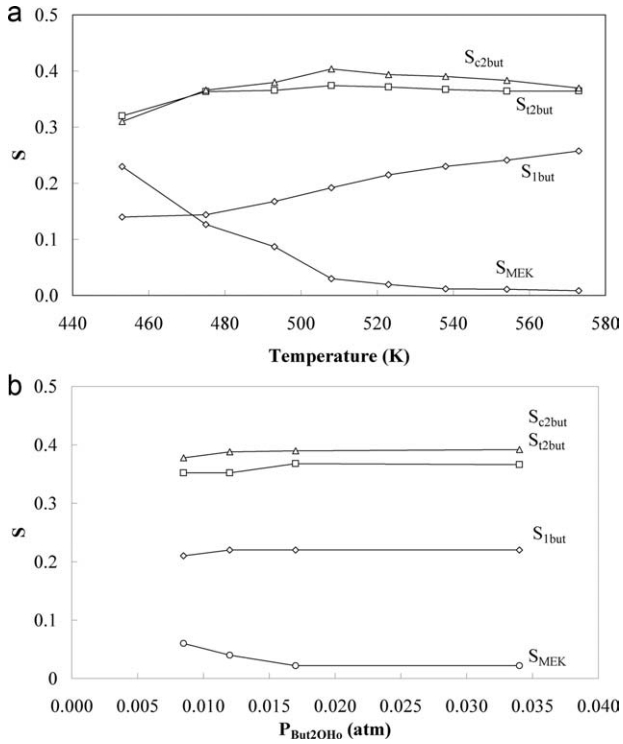

Figure 3. (a) Selectivity of 2-butanol decomposition to different products S_i, as a function of reaction temperature for $W/F_{But2OHo}$ = 0.042 g·s/μmol, and P_{But2OH} = 0.017 atm, (b) Selectivity of 2-butanol decomposition to different products S_i, as a function of 2-butanol inlet partial pressure for T = 523 K, W = 100 mg, and Q = 100 cm^3/min.

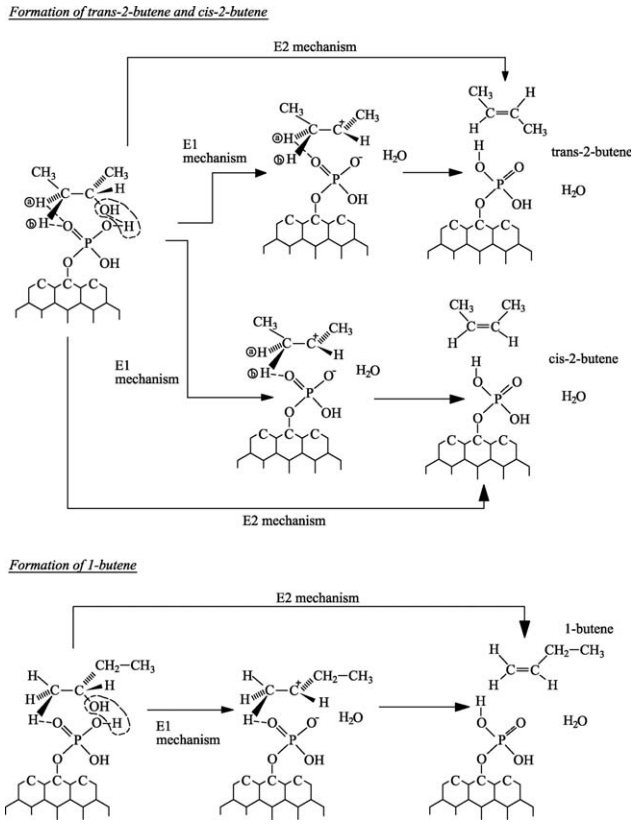

Scheme 1. Formation of 1-butene, trans-2-butene and cis-2-butene from 2-butanol by the two different proposed mechanism.

In both cases two different orientations of adsorbed 2-butanol molecules over a phosphate group of the catalyst surface can occur.

is kinetically controlled. The formation of Saytzeff products (2-olefins) suggests a carbenium ion mechanism of 2-butanol dehydration (E1), where the protogenic surface groups act as proton or hydrogen bridge donors. On the other hand, the formation of 1-butene (Hoffman orientation) suggests a carbanionic mechanism (E1cb). In our case, it is possible to explain the formation of the three olefins by the different orientation of adsorbed 2-butanol molecules over the phosphate group on the surface of the catalyst. Scheme 1 represents the proposed formation mechanism of the olefins from a 2-butanol molecule adsorbed over a phosphate group, which is bonded to the carbon surface through a C-O-P bond.[28,29,30] The formation of the 1-butene or of the isomers trans-2-butene and cis-2-butene is supposed to be determined by the orientation of the adsorbed 2-butanol molecule. The 2-butanol adsorption is supposed to take place by chemisorption of the hydroxyl group of the alcohol molecule over a proton of a phosphate group located on the carbon surface. The adsorbed intermediate can be stabilized by positioning the primary or secondary carbon adjacent to the carbon bonded with the OH group. The fact that the 2-butanol dehydration presents a higher selectivity to the 2-olefin isomers than that of the 1-olefin suggests that the 2-butanol adsorption by the C-OH and the secondary carbon is thermodynamically favored.

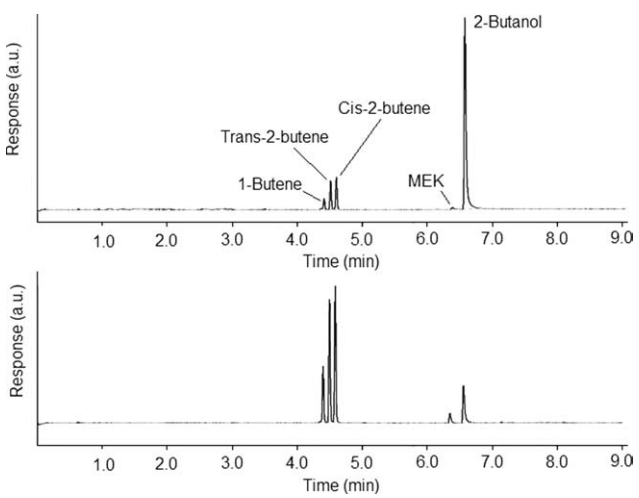

Figure 4. Chromatograms of gas reaction mixture, corresponding to experiments with low (a), and high (b) 2-butanol conversions.

Rigorously, the two adsorption modes should be taken into account in the development of the kinetic model. However, assuming that the heat of adsorption, ΔH, of both possibilities is very similar, both adsorption modes could be

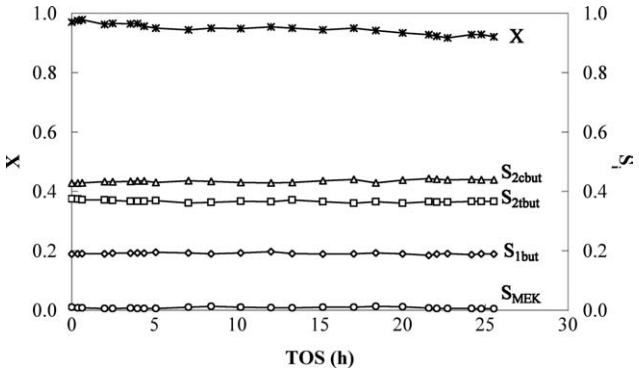

Figure 5. Conversion of 2-butanol and selectivity to different products S_i, as a function of time on stream (TOS) at T = 568 K.

considered as one, simplifying the model resolution. The orientation determines the proton that leaves the alcohol molecule. In the case that this proton belongs to a primary carbon, the formation of the 1-butene occurs, but if the proton that is leaving the alcohol belongs to a secondary carbon the formation of the 2-olefin takes place. The selectivity to trans-2-butene or cis-2-butene depends on which of the two protons bonded to the secondary carbon leaves the alcohol molecules. If the proton (a) (see Scheme 1) is leaving the alcohol trans-2-butene is obtained. However, if the proton that is leaving the molecule is (b) the formation of cis-2-butene takes place. In this case, both protons (a) or (b), have the same probability of leaving the alcohol molecule, and, thus, the selectivity to cis-2-butene or trans-2-butene is very similar (cis/trans = 1.1). The reaction is supposed to occur through two different mechanism, an E1 or E2 elimination mechanisms. E2 concerted mechanism takes place by a single-step in which the alcoholic hydroxyl group and the proton are removed simultaneously. In the E1 elimination mechanism the OH^- group leaves the alcohol first, producing an intermediate carbocation, and the proton leaves it in a second step. In both mechanism, dehydration reaction takes place by deprotonation of the P-OH and protononation of the P = O groups of the phosphate. This implies a rotation of the acidic-basic properties of the oxygen atoms of the phosphate groups, which favors the dehydration reaction. This is stereochemically possible by the bond distances.

The dehydrogenation activity is much lower than the dehydration activity (e.g., 1% of selectivity to mek). Dehydrogenation of alcohol over nonmetal catalyst occurs on Lewis base sites. The basic properties of the activated carbons result from the presence of ionoradical or pyrene-like structures, formed during the activation process or during the thermal stabilization of the activated carbons.

The dehydrogenation and dehydration of 2-butanol are independent of each other because the introduction of mek into the stream of 2-butanol inhibits only the reaction of dehydrogenation.[26]

The evolution of the 2-butanol conversion and selectivities to different products with time on stream (TOS) at 568 K is shown in Figure 5. A very small change in conversion (from 96.8 to 93%), and selectivities is observed for the catalyst after 26 h on stream. The almost negligible carbon catalyst deactivation at the experimental conditions used in this work can be attributed to a very high stability of the surface acidity.

The influence of water vapor in the reaction gas on the catalytic dehydration of 2-butanol was studied. Figure 6 shows the conversion of 2-butanol and selectivities to different products for different inlet partial pressures of water vapor (P_{wo}), at constant inlet 2-butanol partial pressure of 0.017 atm and at 523 K. Despite this catalyst adsorbs a considerable amount of water vapor at room temperature,[28] both conversion and selectivities remained constant for all the experiments, which evidences the high stability of the catalyst to water vapor at the working conditions used. The hydrothermal stability of the catalyst is very important for the valorization of oxygenates since alcohols from biomass precursors are usually obtained with a high-water content in the reaction medium.

2-butanol decomposition kinetics models

Given that the presence of water vapor in the inlet gas stream showed no significant effect in the reaction rate and product selectivities for the carbon catalyst (see Figure 6), the proposed kinetic models assume that the water molecules formed during the dehydration reaction do not adsorb on the catalyst active sites. This water formed in the reaction is probably desorbed rapidly to the gas phase or adsorbed in pores without active sites for the decomposition reaction. Two 2-butanol decomposition (dehydration and dehydrogenation) mechanisms (A and B) have been proposed. The mechanisms differ in the dehydration reaction pathway. In A model the dehydration reaction is supposed to take place by means of an E2 elimination mechanism, while in the B model the dehydration reaction is assumed to occur through an E1 elimination mechanism. In both cases dehydrogenation reaction occurs by an E2 mechanism. The kinetic expressions obtained from both models were used to obtain the kinetic and thermodynamics parameters by numerical optimization of the experimental data.

Two types of active sites have been assumed for both models, one acid site (L) in which the alcohol dehydration takes place and another basic site (L′) in which the dehydrogenation reaction takes place.[60] Both mechanisms

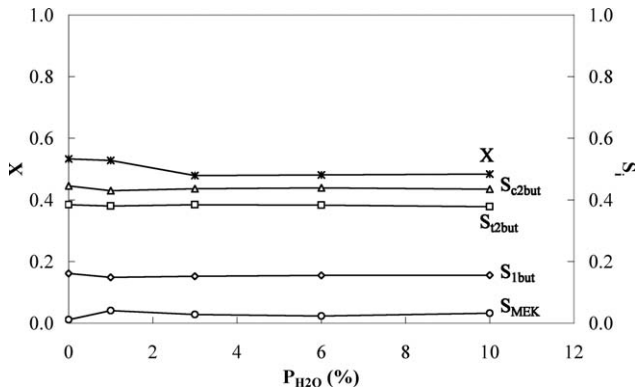

Figure 6. Conversion of 2-butanol and selectivity to different products S_i, as a function of inlet water vapor partial pressure (T = 523 K, W = 100 mg, $P_{But2OHo}$ = 0.017 atm, Q = 100 cm^3/min).

assumed steps of adsorption on the active sites, surface reactions and desorption of the reaction product from the active sites. Besides, in the adsorption step a quasi-equilibrium state is supposed to be reached for both active sites, acid and basic.

The following suppositions were assumed: the reactor is considered as a plug flow integral reactor, homogeneous distribution of active sites on the catalyst surface, catalyst is assumed to operate at steady-state conditions, diffusional constraints and transport limitations were negligible (as theoretically proven before), and changes in temperature and pressure within the reactor were neglected.

A model: E2 elimination mechanism for dehydration and E2 elimination mechanism for dehydrogenation

This model supposed that both dehydration and dehydrogenation reactions occur by an E2 mechanism in a single step that is the rate-determining step. The desorption of the formed olefins is assumed to be fast. Therefore, the olefins were not adsorbed on the dehydration acid sites and the olefin desorption step has no effect in the kinetic expression. However, according to the literature,[26] mek molecules formed by the dehydrogenation reaction are adsorbed in the basic sites, and, therefore, decrease the number of basic sites available for the dehydrogenation reaction, which have to be taken into account in the basic sites balance. A model kinetic expression is shown as follows.

The A model is presented by the following mechanism

Adsorption

$$\mathrm{But2OH(g)} + \mathrm{L} \overset{K_{\mathrm{L}}}{\longleftrightarrow} \mathrm{But2OH - L} \tag{1}$$

$$\mathrm{But2OH(g)} + \mathrm{L'} \overset{K_{\mathrm{L'}}}{\longleftrightarrow} \mathrm{But2OH - L'} \tag{2}$$

Surface reaction

$$\mathrm{But2OH - L} \overset{k_{\mathrm{c2but}}}{\longrightarrow} \mathrm{c2but - L + H_2O(g)} \tag{3}$$

$$\mathrm{But2OH - L} \overset{k_{\mathrm{t2but}}}{\longrightarrow} \mathrm{t2but - L + H_2O(g)} \tag{4}$$

$$\mathrm{But2OH - L} \overset{k_{\mathrm{1but}}}{\longrightarrow} \mathrm{1but - L + H_2O(g)} \tag{5}$$

$$\mathrm{But2OH - L'} \overset{k_{\mathrm{mek}};K_{\mathrm{mek}}}{\longleftrightarrow} \mathrm{mek - L' + H_2(g)} \tag{6}$$

Desorption

$$\mathrm{c2but - L} \overset{1/K_{\mathrm{c2but}}}{\longleftrightarrow} \mathrm{c2but(g) + L} \tag{7}$$

$$\mathrm{t2but - L} \overset{1/K_{\mathrm{t2but}}}{\longleftrightarrow} \mathrm{t2but(g) + L} \tag{8}$$

$$\mathrm{1but - L} \overset{1/K_{\mathrm{1but}}}{\longleftrightarrow} \mathrm{1but(g) + L} \tag{9}$$

$$\mathrm{mek - L'} \overset{1/K_{\mathrm{AL'}}}{\longleftrightarrow} \mathrm{mek(g) + L'} \tag{10}$$

The mass balance for all the adsorbed species over the active sites leads to the following rate expressions

Table 2. Calculated Kinetic Parameters from the Two Models Used

	k_{io}, K_{io}	E_{ai}, ΔH_i (kJ/mol)
A model		
K_{L}	$5.03\cdot10^{-1} \pm 1.96\cdot10^{-2}$	-24.54 ± 0.17
k'_{c2but}	$2.17\cdot10^{+2} \pm 3.85$	77.17 ± 0.08
k'_{t2but}	$2.50\cdot10^{+2} \pm 5.12$	78.10 ± 0.09
k'_{1but}	$2.34\cdot10^{+3} \pm 5.52\cdot10^{+1}$	90.18 ± 0.10
$K_{\mathrm{L'}}$	$7.59\cdot10^{-2} \pm 1.03\cdot10^{-3}$	-29.52 ± 0.47
K_{mek}	$1.24\cdot10^{-2} \pm 2.58\cdot10^{-3}$	19.89 ± 6.71
k_{mek}	$1.59\cdot10^{+3} \pm 1.08\cdot10^{+1}$	78.88 ± 0.30
$K_{\mathrm{AL'}}=1/K_{\mathrm{D}}$	$1.89\cdot10^{-1} \pm 3.45\cdot10^{-2}$	-37.93 ± 6.68
Residual as	$\sum_i \left(X_i^{\mathrm{exp}} - X_i^{\mathrm{cal}}\right)^2$	$2.945\cdot10^{-2}$
B model		
K_{L}	$6.76\cdot10^{-1} \pm 2.88\cdot10^{-2}$	-23.29 ± 0.19
$k'_{\mathrm{2but+}}$	$9.44\cdot10^{+2} \pm 1.83\cdot10^{+1}$	79.64 ± 0.09
k'_{c2but}	$9.90\cdot10^{+5} \pm 7.60\cdot10^{+4}$	79.05 ± 5.22
k'_{t2but}	$1.14\cdot10^{+6} \pm 8.76\cdot10^{+4}$	79.97 ± 5.23
k'_{1but}	$1.06\cdot10^{+7} \pm 8.44\cdot10^{+5}$	92.03 ± 5.22
$K_{\mathrm{L'}}$	$1.30\cdot10^{-1} \pm 2.60\cdot10^{-3}$	-29.72 ± 0.83
K_{mek}	$3.00\cdot10^{-3} \pm 6.45\cdot10^{-4}$	19.69 ± 7.64
k_{mek}	$1.59\cdot10^{+3} \pm 8.50\cdot10^{+1}$	78.92 ± 0.87
$K_{\mathrm{AL'}}=1/K_{\mathrm{D}}$	$9.03\cdot10^{-2} \pm 2.54\cdot10^{-2}$	-37.72 ± 7.57
Residual as	$\sum_i \left(X_i^{\mathrm{exp}} - X_i^{\mathrm{cal}}\right)^2$	$2.950\cdot10^{-2}$

$$r_i = k_i \cdot C_{\mathrm{Lo}} \cdot \theta_{(\mathrm{But2OH-L})} = k'_i \frac{K_{\mathrm{L}} \cdot P_{\mathrm{But2OH}}}{1 + K_{\mathrm{L}} \cdot P_{\mathrm{But2OH}}} \qquad \mathrm{i: c2but, t2but, 1but} \tag{11}$$

$$r_{\mathrm{mek}} = k_{\mathrm{mek}} \cdot C_{\mathrm{L'o}} \cdot \theta_{\mathrm{But2OH-L'}} = \frac{k'_{\mathrm{mek}} K_{\mathrm{L'}} \cdot \left(P_{\mathrm{But2OH}} - \frac{P_{\mathrm{mek}} P_{\mathrm{H_2}}}{K_{\mathrm{L'}} K_{\mathrm{mek}} K_{\mathrm{D}}}\right)}{1 + K_{\mathrm{L'}} \cdot P_{\mathrm{But2OH}} + \frac{P_{\mathrm{mek}}}{K_{\mathrm{D}}}} \tag{12}$$

$$-r_{\mathrm{But2OH}} = r_{\mathrm{c2but}} + r_{\mathrm{t2but}} + r_{\mathrm{1but}} + r_{\mathrm{mek}} \tag{13}$$

B model: E1 elimination mechanism for dehydration and E2 elimination mechanism for dehydrogenation

In this case, dehydration reaction is assumed to take place by an E1 mechanism through two successive steps, (1) the formation of the intermediate carbocation and loss of the water molecule, and (2) the formation of the olefin isomers. The minority dehydrogenation reaction is assumed to occur, like for A model, by an E2 mechanism in a single step. The carbocation formation is assumed to be in a pseudo-steady state. Like for A model, the desorption of the olefins is assumed to be fast, and, therefore, it was not considered in the acid site balance. Based on the literature,[26] mek is supposed to be adsorbed on the basic sites and it was considered in the basic site balance. The kinetic expression of the B model is shown.

B model is represented by the following mechanism

Adsorption

$$\mathrm{But2OH(g)} + \mathrm{L} \overset{K_{\mathrm{L}}}{\longleftrightarrow} \mathrm{But2OH - L} \tag{1}$$

$$\mathrm{But2OH(g)} + \mathrm{L'} \overset{K_{\mathrm{L'}}}{\longleftrightarrow} \mathrm{But2OH - L'} \tag{2}$$

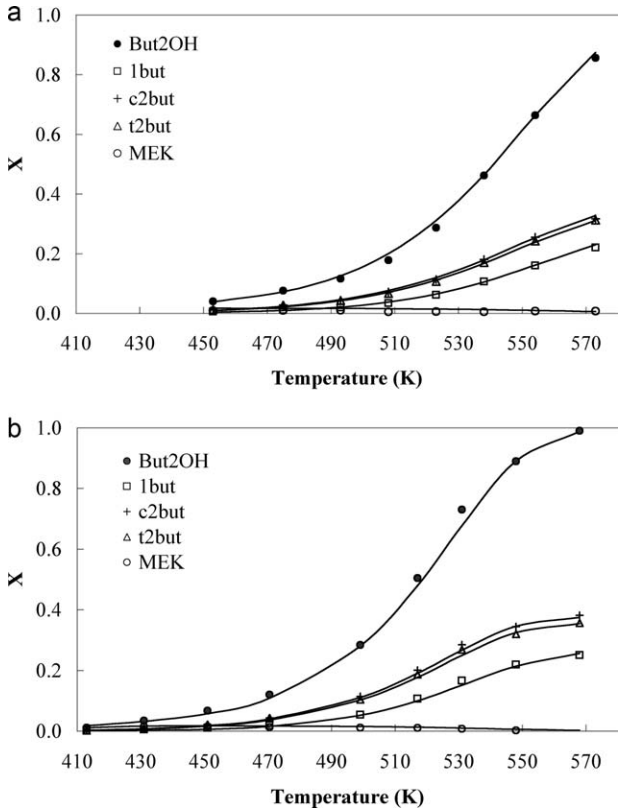

Figure 7. Steady-state conversion of 2-butanol and yield to different reaction products for $P_{But2OHo}$ = 0.017 atm and space-times of (a) 0.042 and (b) 0.085 g·s/μmol (symbols: experimental values, lines: calculated values).

Superficial reaction

$$\mathrm{But2OH-L} \xrightarrow{k_{2but^+}} 2but^+ - \mathrm{L} + \mathrm{H_2O(g)} \quad (14)$$

$$2but^+ - \mathrm{L} \xrightarrow{k_{c2but}} \mathrm{c2but-L} \quad (15)$$

$$2but^+ - \mathrm{L} \xrightarrow{k_{t2but}} \mathrm{t2but-L} \quad (16)$$

$$2but^+ - \mathrm{L} \xrightarrow{k_{1but}} \mathrm{1but-L} \quad (17)$$

$$\mathrm{But2OH-L'} \overset{k_{mek};K_{mek}}{\longleftrightarrow} \mathrm{mek-L'} + \mathrm{H_2(g)} \quad (6)$$

Desorption

$$\mathrm{c2but-L} \overset{1/K_{c2but}}{\longleftrightarrow} \mathrm{c2but(g)} + \mathrm{L} \quad (7)$$

$$\mathrm{t2but-L} \overset{1/K_{t2but}}{\longleftrightarrow} \mathrm{t2but(g)} + \mathrm{L} \quad (8)$$

$$\mathrm{1but-L} \overset{1/K_{1but}}{\longleftrightarrow} \mathrm{1but(g)} + \mathrm{L} \quad (9)$$

$$\mathrm{mek-L'} \overset{1/K_{AL'}}{\longleftrightarrow} \mathrm{mek(g)} + \mathrm{L'} \quad (10)$$

The mass balance of the adsorbed species over the active sites leads to the following rate expressions

$$r_{2but^+-L} = \frac{d\theta_{2but^+-L}}{dt} = k'_{2but^+} \cdot \theta_{But2OH-L} - \left(k'_{c2but} + k'_{t2but} + k'_{1but}\right) \cdot \theta_{2but^+-L} \approx 0 \quad (18)$$

$$r_i = k_i \cdot C_{Lo} \cdot \theta_{2but^+-L} = k'_i \frac{\frac{k'_{2but^+-L} \cdot K_L \cdot P_{But2OH}}{\left(k'_{c2but}+k'_{t2but}+k'_{1but}\right)}}{1 + K_L \cdot P_{But2OH} + \frac{k'_{2but^+-L} \cdot K_L \cdot P_{But2OH}}{\left(k'_{c2but}+k'_{t2but}+k'_{1but}\right)}} \quad i: c2but, t2but, 1but \quad (19)$$

$$r_{mek} = k_{mek} \cdot C_{L'o} \cdot \theta_{but2OH-L'} = \frac{k'_{mek} K_{L'} \cdot \left(P_{But2OH} - \frac{P_{mek} P_{H_2}}{K_{L'} K_{mek} K_D}\right)}{1 + K_{L'} \cdot P_{But2OH} + \frac{P_{mek}}{K_D}} \quad (12)$$

$$-r_{But2OH} = r_{c2but} + r_{t2but} + r_{1but} + r_{mek} \quad (13)$$

The dependence of the kinetic and thermodynamic parameters with the temperature was considered to follow an Arrhenius law for the kinetic constant (Eq. 20) or a Van't Hoff law for the adsorption constants (Eq. 21)

$$k_i = k_{io} \exp\left(\frac{-E_{ai}}{RT}\right) \quad (20)$$

$$K_i = K_{io} \exp\left(\frac{-\Delta H_i}{RT}\right) \quad (21)$$

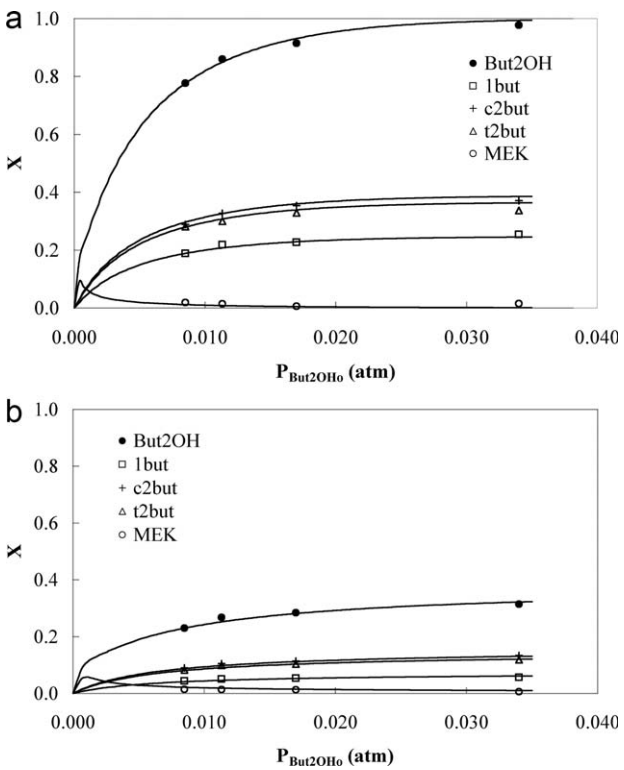

Figure 8. Evolution of 2-butanol conversion and yield to the different products with $P_{But2OHo}$ at a space-time of 0.085 g·s/μmol and at (a) 553, and (b) 499 K (symbols: experimental values, lines: calculated values).

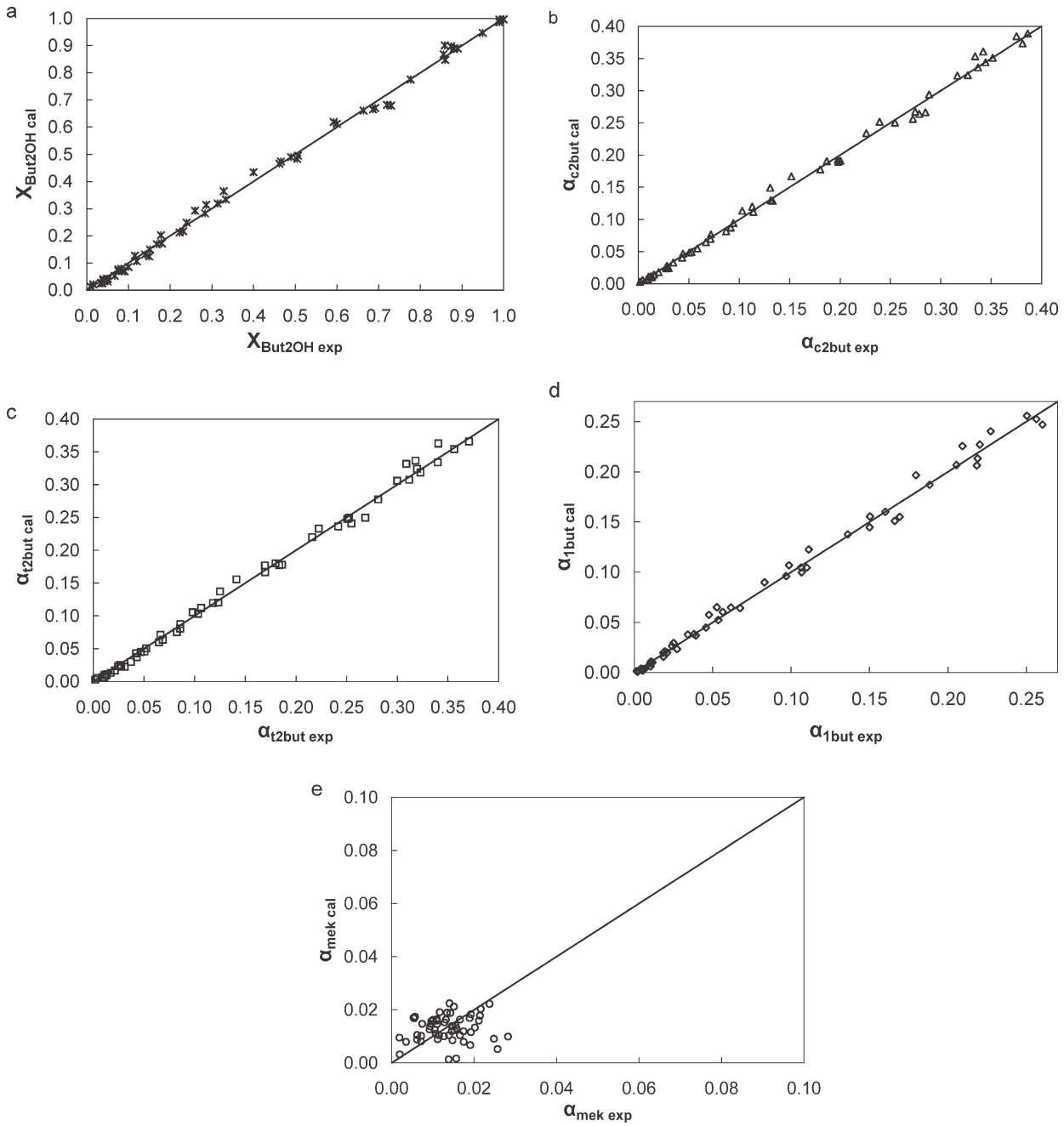

Figure 9. Calculated conversion (obtained by applying B model) vs. experimental for (a) 2-butanol and different reaction products (b) cis-2-butene, (c) trans-2-butene, (d)1-butene, and (e) methyl ethyl ketone.

Combining molar balances, rates equations and stoichiometrics relationships, the following system of differential equations is obtained

$$\left(\frac{W}{F_{\mathrm{But2OHo}}}\right) = -\int_0^{X_{\mathrm{But2OH}}} \frac{\mathrm{d}X_{\mathrm{But2OH}}}{r_{\mathrm{But2OH}}} \tag{22}$$

$$\left(\frac{W}{F_{\mathrm{But2OHo}}}\right) = \int_0^{\alpha_i} \frac{d\alpha_i}{r_i} \qquad i : c2\mathrm{but}, t2\mathrm{but}, 1\mathrm{but}, \mathrm{mek} \tag{23}$$

The parameters involved in the differential equations system were calculated using the Runge-Kuta method, implemented in Matlab 7.0 software, by minimizing the objective function

$$\chi = \sum_i \left(X_i^{\mathrm{exp}} - X_i^{\mathrm{cal}}\right)^2 \tag{24}$$

were X_i^{exp} represents the value of the conversion obtained experimentally, and X_i^{cal} the calculated value. The optimization routine was based in the Levenberg-Marquart algorithm. This optimization problem was solved individually for each model. The values obtained for the kinetics parameters, with

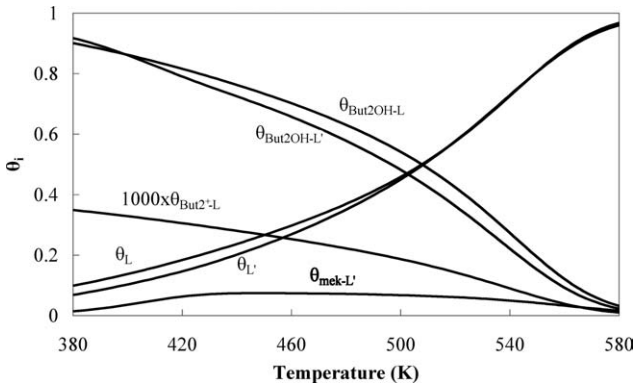

Figure 10. Amount of acid and basic free sites and fractional coverage for the different adsorbed species as a function of the reaction temperature obtained by B model (0.0085 atm, 0.085 g·s/μmol).

95% confidence interval, using the two models are presented in Table 2.

The low residual values for the A and B models ($\chi \approx 0.027$) indicate that both models simulated properly the experimental data. This suggests that both mechanism (E1 and E2) may take place simultaneously during the 2-butanol dehydration reaction. This assumption was previously stated by other authors[14,60] based on the product distribution. In our case, this supposition is supported by the similar rate constant obtained for the formation of the carbocation (k'_{2but+}) in the B model and by the formation of the olefins (k'_{c2but}, k'_{t2but}, k'_{1but}) in the A model. If the rate constants for the olefins formation obtained by applying the B model were compared with those obtained by the A model, it can be observed that the former are higher because in this case the determining rate step is the carbocation formation. This result indicates that formation of the carbocation through an E1 mechanism, and the formation of the cis-2-butene, trans-2-butene and 1-butene by an E2 mechanism occur at a very similar rate, and, therefore, it is probably that both mechanisms take place simultaneously. As the concerted mechanism is truly synchronous only in exceptional cases, the reaction is supposed to occur as E2 with strong E1 character.[14]

Figure 7a and b represent the total conversion of 2-butanol and the yield to the different reaction products at an inlet partial pressure of 2-butanol of 0.017 atm and space-times of 0.042 and 0.085 g·s/μmol, respectively. The solid lines represent the conversion obtained from B model. The model simulated fairly well the experimental values for both the total 2-butanol conversion and the yield to the different products. The simulation with the A model (not shown) is likewise properly. The comparison of both Figure reveals that at a constant inlet 2-butanol partial pressure, the increase of the space-time leads to higher conversion values.

Figure 8a and b show the evolution of 2-butanol conversion and the yield to the different products with the inlet 2-butanol partial pressure for space-time of 0.085 g·s/μmol, at 553 and 499 K, respectively. The solid line represents the simulated conversion estimated by applying B model. An increase in the inlet 2-butanol partial pressures produces a slight increase in the selectivity to the dehydration products, 1-butene, cis-2-butene and trans-2-butene, and a decrease in the selectivity to the dehydrogenation product, mek.

The quality of the fitting of B model can be observed in Figure 9a to e. This figure represents the conversion simulated vs. the conversion obtained experimentally for the 2-butanol decomposition and cis-2-butene, trans-2-butene, 1-butene and mek formation, respectively, on the carbon catalyst. A proper fitting of the model to the experimental data is observed in the figure; only mek shows a slight deviation due to the low selectivities to this product that may be strongly affected by the experimental low-yield values.

Figure 10 represents the estimated evolution of the amount of acid and basic free sites and the fractional coverage, obtained by B model, as a function of the reaction temperature. The amount of acid and basic free sites increases with the reaction temperature as conversion increases due to the increase in the reaction rate. The fractional coverage of the carbocation is very low and decreases with the reaction temperature. A similar result has been obtained for the A model.

Conclusions

The chemical activation of olive stone residues with H_3PO_4 results in an activated carbon with a high-surface acidity because of the residual phosphorus that remains in the carbon surface. The carbon obtained show a well developed microporous structure. The XPS P2p spectra of the activated carbons show contribution of C-O-PO_3 and C-PO_3 groups.

Conversion of 2-butanol yields mainly dehydration products, mostly cis-2-butene and trans-2-butene with lower amounts of 1-butene, and a very small amount of mek as dehydrogenation product. Kinetic interpretation of the experimental data was performed using two elimination mechanisms for the dehydration reaction; an E1 mechanism (two-step mechanism), and an E2 mechanism (one-step mechanism). The rate expressions derived from both models fit properly the experimental results, suggesting that probably the two mechanisms occur simultaneously. This supposition is supported by the similar rate constant obtained for the formation of the carbocation in the E1 mechanism and for the formation of the olefins in the E2 mechanism. This fact indicates that formation of the carbocation through an E1 mechanism and the formation of the cis-2-butene, trans-2-butene and 1-butene by an E2 mechanism occur at a very similar rate, and, therefore, it is probably that both mechanisms take place simultaneously.

Acknowledgments

The authors thank the Ministry of Science and Education of Spain for financial support (DGICYT, Projects CTQ06/11322 and NAN04/09312-C03-03). J.B. acknowledges the assistance of the Ministry of Science and Education of Spain for the award of a FPI grant.

Notation

A_{BET}^{N2} = apparent surface area obtained by the BET method, $m^2 \cdot g^{-1}$
A_{DR}^{CO2} = apparent area of narrow micropores, $m^2 \cdot g^{-1}$

A_t^{N2} = external area obtained by the t method, $m^2 \cdot g^{-1}$
BET = Brunauer, Emmett, and Teller
1but = 1-butene
But2OH = 2-butanol
c2but = cis-2-butene
C_{Lo}, $C_{L'o}$ = total active site concentration, $\cdot g^{-1}$
Da = Damköhler number
d_p = particle diameter
DR = Dubinin-Radushkevich
E_a = activation energy, $kJ \cdot mol^{-1}$
$F_{But2OHo} = F_{to} \cdot P_{But2OHo}$ = initial molar flow of 2-butanol, $mol \cdot s^{-1}$
ΔH_i = adsorption enthalpy of component i, $kJ \cdot mol^{-1}$
i-L = component i bonded to L site, But2OH-L; c2but-L; t2but-L; 1but-L; $2but^+$-L
i-L′ = component i bonded to L′ site, But2OH-L′; mek-L′
k_j = reaction j intrinsic kinetic constant
$k_j' = k_j \cdot C_{Lo}$ = reaction j apparent kinetic constant
k_{jo} = preexponential factor of Ahrrenius equation, reaction j.
$K_{AL'}$ = adsorption equilibrium constant for mek in L′ site.
K_D = desorption equilibrium constant for mek in L′ site, $(1/K_{AL'})$.
K_L = adsorption equilibrium constant for 2-butanol in L site
$K_{AL'}$ = adsorption equilibrium constant for 2-butanol in L′ site
K_{mek} = equilibrium constant for the 2-butanol dehydrogenation reaction to mek
L = acid site
L′ = basic site
L_b = bed length
mek = methyl-ethyl-ketone
NDIR = nondispersive infrared
P_{io} = component i initial pressure, atm
P_i = component i final pressure, atm
R = universal gas constant, $J \cdot mol^{-1} \cdot K^{-1}$
r_i = rate equation for component i
S_i = selectivity to i product
STP = standard temperature-pressure conditions
t2but = trans-2-butene
TOS = time on stream
TPD = temperature-programmed desorption
V_{DR}^{CO2} = micropore volume obtained by the DR method, $cm^3 \cdot g^{-1}$
V_{mes}^{N2} = mesopore volume, $cm^3 \cdot g^{-1}$
V_{mic}^{N2} = micropore volume obtained by the t method, $cm^3 \cdot g^{-1}$
W = weight of catalyst, g
$X_{But2OH} = \frac{P_{But2OHo} - P_{But2OH}}{P_{But2OHo}}$ = 2-butanol conversion
XPS = X-ray photoelectron spectroscopy

Greek letters

$\alpha_i = \frac{P_i}{P_{But2OHo}}$ = 2-butanol conversion to i product
η = internal effectiveness factor
η_{ext} = external effectiveness factor
ϕ = Thiele modulus
χ = objective function (Residual error)
θ_L = free superficial fraction coverage of L site
$\theta_{L'}$ = free superficial fraction coverage of L′ site
θ_{i-L} = superficial fraction coverage of L site occupied by i product
$\theta_{i-L'}$ = superficial fraction coverage of L′ site occupied by i product

Literature Cited

1. Branca C, Giudicianni P, Di Blasi C. GC/MS Characterization of liquids generated from low-temperature pyrolysis of wood. *Ind Eng Chem Res*. 2003;42:3190–3202.
2. Pütün AE, Özcan A, Gerçel HF, Pütün E. Production of biocrudes from biomass in a fixed-bed tubular reactor: product yields and compositions. *Fuel*. 2001;8:1371–1378.
3. Adjaye JD, Katikaneni SPR, Bakhshi NN. Catalytic conversion of a biofuel to hydrocarbons: effect of mixtures of HZSM-5 and silica-alumina catalysts on product distribution. *Fuel Process Technol*. 1996;48:115–143.
4. Gayubo AG, Aguayo AT, Atutxa A, Aguado R, Bilbao J. Transformation of oxygenate components of biomass pyrolysis oil on a HZSM-5 Zeolite. I. Alcohols and phenols. *Ind Eng Chem Res*. 2004;43:2610–2618.
5. Gayubo AG, Aguayo AT, Atutxa A, Aguado R, Olazar M, Bilbao J. Transformation of oxygenate components of biomass pyrolysis oil on a HZSM-5 Zeolite. II. Aldehydes, ketones, and acids. *Ind Eng Chem Res*. 2004;43:2619–2626.
6. Abu-Zied BM. Structural and catalytic activity studies of silver/chromia catalysts. *Appl Catal A*. 2000;198:139–153.
7. Millar GJ, Nelson ML, Uwins PJR. In Situ imaging of catalytic etching on silver during methanol oxidation conditions by environmental scanning electron microscopy. *J Catal*. 1997;169:143–156.
8. Quaranta NE, Soria J, Corberán VC, Fierro JLG. Selective oxidation of ethanol to acetaldehyde on $V_2O_5/TiO_2/SiO_2$ catalysts. *J Catal*. 1997;171:1–13.
9. Gines MJL, Iglesia E. Bifunctional condensation reactions of alcohols on basic oxides modified by copper and potassium. *J Catal*. 1998;176:155–172.
10. van de Water LGA, van der Waal JC, Cansen JC, Maschmeyer T. Improved catalytic activity upon Ge incorporation into ZSM-5 zeolites. *J Catal*. 2004;223:170–178.
11. Tejero J, Fité C, Iborra M, Izquierdo JF, Cunill F, Bringué R. Liquid-phase dehydrocondensation of 1-pentanol to di-n-pentyl ether (DNPE) over medium and large pore acidic zeolites. *Microp Mesop Mats*. 2009;117:650–660.
12. Tejero J, Cunill F, Iborra M, Izquierdo JF, Fité C. Dehydration of 1-pentanol to di-n-pentyl ether over ion-exchange resin catalysts. *J Mol Catal A*. 2002;182–183:541–554.
13. Bringué R, Iborra M, Tejero J, Izquierdo JF, Cunill F, Fité C. Cruz VJ. Thermally stable ion-exchange resins as catalysts for the liquid-phase dehydration of 1-pentanol to di-n-pentyl ether (DNPE). *J Catal*. 2006;244:33–42.
14. Delsarte S, Grange P. Butan-1-ol and butan-2-ol dehydration on nitrided aluminophosphates: influence on nitridation on reaction pathways. *Appl Catal A*. 2004;259:269–279.
15. Aramendia MA, Borau V, Jiménez C, Marinas JM, Porras A, Urbano FJ. Magnesium oxides as basic catalysts for organic processes. Study of the dehydrogenation-dehydration of 2-propanol. *J Catal*. 1996;161:829–838.
16. Iglesia E, Barton DG, Biscardi JA, Gines MJL, Soled SL. Bifunctional pathways in catalysis by solid acids and bases. *Catal Today*. 1997;38:339–360.
17. Hattori H. Heterogeneous basic catalysis. *Chem Rev*. 1995;95:537–558.
18. Radovic LR, Rodríguez-Reinoso F. In: Thrower PA. *Chemistry and Physics of Carbon*. Vol. 25. New York: Marcel Dekker; 1997:243–358.
19. Radovic LR, Sudhakar C. *Introduction to Carbon Technologies*. Marsh H, Heintz EA, Rodríguez-Reinoso F, eds. Secretariado de Publicaciones, Universidad de Alicante, Alicante, Spain; 1997:107.
20. Rodríguez-Reinoso F. The role of carbon materials in heterogeneous catalysis. *Carbon*. 1998;36:159–175.
21. Leon y Leon CA, Radovic LR. In: Thrower PA, ed. *Chemistry and Physics of Carbon*. New York: Marcel Dekker; 1992:213–310.
22. Szymański GS, Rychlicki G. Catalytic conversion of propan-2-ol on carbon catalysts. *Carbon*. 1993;31:247–257.
23. Moreno-Castilla C, Pérez-Cadenas AF, Maldonado-Hódar FJ, Carrasco-Marín F, Fierro JLG. Influence of carbon-oxygen surface complexes on the surface acidity of tungsten oxide catalysts supported on activated carbons. *Carbon*. 2003;41:1157–1167.
24. Moreno-Castilla C, Carrasco-Marín F, Parejo-Pérez C, López Ramón MV. Dehydration of methanol to dimethyl ether catalyzed by oxidized activated carbons with varying surface acidic character. *Carbon*. 2001;39:869–875.
25. Carrasco-Marín F, Mueden A, Moreno-Castilla C. Surface-treated activated carbons as catalysts for the dehydration and dehydrogenation reactions of ethanol. *J Phys Chem B*. 1998;102:9239–9244.

26. Szymanski GS, Rychlicki G. Importance of oxygen surface groups in the catalytic dehydration and dehydrogenation of butan-2-ol promoted by carbon catalysts. *Carbon*. 1991;29:489–498.
27. Figueiredo JL, Pereira MFR, Freitas MMA, Orfao JJM. Modification of the surface chemistry of activated carbons. *Carbon*. 1999;37: 1379–1389.
28. Rosas JM, Bedia J, Rodríguez-Mirasol J, Cordero T. Preparation of hemp-derived activated carbon monoliths. Adsorption of water vapour. *Ind Eng Chem Res*. 2008;47:1288–1296.
29. Rosas JM, Bedia J, Rodríguez-Mirasol J, Cordero T. HEMP-derived activated carbon fibers by chemical activation with phosphoric acid. *Fuel*. 2009;88:19–26.
30. Bedia J, Rosas JM, Márquez J, Rodríguez-Mirasol J, Cordero T. Preparation and characterization of carbon based acid catalysts for the dehydration of 2-propanol. *Carbon*. 2009;47:286–294.
31. Costa E, Uguina A, Aguadi J, Hernández PJ. Ethanol to gasoline process: effect of variables, mechanism, and kinetics. *Ind Eng Chem Process Des Des*. 1985;24:239–245.
32. González-Serrano E, Cordero T, Rodríguez-Mirasol J, Cotoruelo L, Rodríguez JJ. Removal of water pollutants with activated carbons prepared from H_3PO_4 activation of lignin from kraft black liquors. *Water Res*. 2004;38:3043–3050.
33. Brunauer S, Emmett PH, Teller E. Adsorption of gases in multimolecular layers. *J Am Chem Soc*. 1938;60:309–319.
34. Lippens BC, de Boer JH. Studies on pore systems in catalysts V. The t method. *J Catal*. 1965;4:319–323.
35. Rodríguez-Reinoso F, Molina-Sabio M, González MT. The use of steam and CO_2 as activating agents in the preparation of activated carbons. *Carbon*. 1995;33:15–23.
36. Dubinin MM, Zaverina ED, Radushkevich LV. Sorption and structure of active carbons. I. Adsorption of organic vapors. *J Phys Chem* (URSS). 1947;21:1351–1362.
37. Gregg SJ, Sing KSW. *Adsorption Surface Area and Porosity*. London: Academic Press; 1982.
38. Rodríguez-Reinoso F. *Carbon and Coal Gasification*. In: Figueireido JL, Moulijn JA. Dordretch, eds. The Netherlands: Martinus Nijhoff Plubishers; 1986.
39. Biniak S, Szymanski G, Siedlewski J, Swiatkowski A. The characterization of activated carbons with oxygen and nitrogen surface groups. *Carbon*. 1997;35:1799–1810.
40. Desimoni E, Casella GI, Morone A, Salvi AM. XPS determination of oxygen containing functional groups on carbon-fibre surfaces and the cleaning of these surfaces. *Surf Interface Anal*. 1990;15:627–634.
41. Aramendia MA, Borau V, Jiménez C, Marinas JM, Romero FJ, Urbano FJ. Microemulsion-assisted synthesis of catalysts based on aluminium and magnesium phosphates. *J Mol Catal A*. 2002;35: 182–183.
42. Parida KM, Acharya M, Mishra T. Tungstate-modified aluminium phosphate: 1. Preparation, characterisation and catalytic activity towards alcohol and cumene conversion reactions. *J Mol Catal A*. 2000;164:217–223.
43. Rodríguez-Mirasol J, Cordero T, Rodríguez JJ. Activated carbons from CO_2 partial gasification of eucalyptus kraft lignin. *Energy Fuels*. 1993;7:133–138.
44. Suárez-García F, Martínez-Alonso A, Tascón JMD. Activated carbon fibers from Nomex by chemical activation with phosphoric acid. *Carbon*. 2004;42:1419–1426.
45. Jagtoyen M, Derbyshire F. Some considerations of the origins of porosity in carbons from chemically activated wood. *Carbon*. 1993; 31:1185–1192.
46. Puziy AM, Poddubnaya OI, Martínez-Alonso A, Suárez-García F, Tascón JMD. Synthetic carbons activated with phosphoric acid: I. Surface chemistry and ion binding properties. *Carbon*. 2002;40: 1493–505.
47. Puziy AM, Poddubnaya OI, Martínez-Alonso A, Suárez-García F, Tascón JMD. Surface chemistry of phosphorus-containing carbons of lignocellulosic origin. *Carbon* 2005;43:2857–68.
48. Wu X, Radovic LR. Inhibition of catalytic oxidation of carbon/carbon composites by phosphorus. *Carbon*. 2006;44:141–151.
49. Bansal RC, Donnet JB, Stoeckli F. *Active Carbon*. New York: Marcel Dekker, 1988.
50. Cordero T, Rodríguez-Mirasol J, Tancredi N, Piriz J, Vivo G, Rodríguez JJ. Influence of surface composition and pore structure on Cr (III) adsorption onto activated carbons. *Ind Eng Chem Res*. 2002; 41:6042–6048.
51. Hall PJ, Calo JM, Teng H, Suuberg EM, May JA, Lilly WD. The nature of carbon-oxygen complexes produced by different oxidants: towards a unified theory of gasification?. *Prepr Pap Am Chem Soc, Div Fuel Chem*. 1989;34:112–121.
52. Ichikawa N, Sato S, Takahashi R, Sodesawa T. Catalytic reaction of 1,3-butanediol over solid acids. *J Mol Catal A*. 2006;256:106–112.
53. Aguayo AT, Gayubo AG, Vivanco R, Olazar M, Bilbao J. Role of acidity and microporous structure in alternative catalysts for the transformation of methanol into olefins. *Appl Catal A*. 2005;283: 197–207.
54. Mears DE. The role of axial dispersion in trickle-flow laboratory reactors. *Chem Eng Sci*. 1971;26:1361–1366.
55. Satterfield CN. *Heterogeneous Catalysis in Practice*. New York: McGraw-Hill; 1991.
56. Moulijn JA, Tarfaoui A, Kapteijn F. General aspects of catalyst testing. *Catal Today*. 1991;11:1–12.
57. Vannice MA. *Kinetics of Catalytic Reactions*. Springer; 2005:51–61.
58. Knozinger H, Khone R. The dehydration of alcohols over alumina: I. The reaction scheme. *J Catal*. 1996;5:264–270.
59. Knozinger H, Buhl H, Kochloefl K. The dehydration of alcohols on alumina: XIV. Reactivity and mechanism. *J Catal*. 1972;24:57–68.
60. López T, Gomez R, Llanos ME, López-Salinas E. Acidic-base properties of silica- magnesia sol-gel mixed oxides: use of 2-butanol as test reaction. *Mater Lett*. 1999;38:283–288.

Manuscript received Feb. 28, 2009, and revision received Aug. 1, 2009.